Occupancy Fluctuation Effects on 3D Hubbard Model at Quarter Filling within Dynamical Mean-Field Theory

IOP Conf. Series: Materials Science and Engineering **515** (2019) 012011 doi:10.1088/1757-899X/515/1/012011

Occupancy Fluctuation Effects on 3D Hubbard Model at Quarter Filling within Dynamical Mean-Field Theory

N. A. Tadjuddin, C. N. Rangkuti, M. A. Majidi*

Department of Physics, Faculty of Mathematics and Natural Sciences, Universitas Indonesia, Depok 16424, Indonesia

*Corresponding author's email: aziz.majidi@sci.ui.ac.id

Abstract. Research on materials classified into strongly-correlated systems has become a crucial subject due to the strong interactions among the material constituents yielding various exotic physical properties and phenomena. There have been many computational methods developed to address the properties of such systems accurately within the Hubbard model, but most of them require a lot of computational costs to expect good results. In this research, we proposed a new approach within the Dynamical Mean Field Theory (DMFT) framework that requires a simpler and potentially less numerical-cost algorithm. We implemented this algorithm by constructing the local self-energy matrix elements that depend on the occupancy fluctuations. We integrated them over all possible occupancy configurations to obtain the fully interacting Green functions. The resulted Green function matrix was then used to compute the density of states (DOS) and other quantities. We investigated the case of quarter filling. Our computation results showed that pseudogap appeared when the onsite Coulomb repulsion was sufficiently high and tended to diminish as temperature increased. The system preserved its paramagnetic metallic character for all circumstances we studied.

Keywords: Hubbard model, quarter filling, dynamical mean field theory, DOS

1. Introduction

The strongly-correlated system is a condensed-matter system in which the constituent particles strongly interact with one another directly or indirectly yielding exotic physical properties and phenomena that depend on temperature, pressure, doping level, and other factors. Among the notable phenomena emerging in this system are, for instance, Mott-Hubbard metal-insulator transition [1] and charge ordering where the charges tend to localize on different sites due to the strong on-site electron-electron interactions [2,3]. In this regard, nowadays, the Hubbard model is believed to provide a way to explain how the interaction among electrons gives rise to such phenomena. Despite its simplicity, the Hubbard model has proven that it is capable of capturing many of the most subtle and fascinating properties of solid state systems [4].

Numerous computational methods have been developed to address the properties of the strongly-correlated systems accurately within the Hubbard model. However, most of them require a lot of computational costs to expect good results. For instance, the use of exact diagonalization technique is limited by the exponential growth of the computation time with system size, while, Quantum Monte

Carlo method usually faces the minus-sign problem at low temperatures [5]. On the contrary, mean field theory (MFT) offers low numerical cost but has several drawbacks as the method completely freezes both spatial and local quantum fluctuations. Beyond MFT, dynamical mean field theory (DMFT) provides an approximation to privilege these fluctuations by treating them from the beginning in a non-perturbative manner [6]. Related to the aforementioned issue, we aimed to propose a new approach within the DMFT framework that requires a simpler and potentially less numerical-cost algorithm that can still manage to explain the occupancy fluctuation effects. This new DMFT algorithm treats occupancy fluctuations as classical quantities. The idea is motivated by similar treatment of the semiclassical DMFT implementation for electron-phonon coupling [7]. To evaluate the performance of this algorithm, here we address the behavior of three-dimensional Hubbard model at a quarter filling by inspecting how the corresponding DOS evolves as a function of the on-site Coulomb repulsion U and temperature T.

2. Methods

2.1 Model

As described earlier, we wished to study the three-dimensional Hubbard model at a quarter filling. To accommodate the possibility of staggered orderings such as charge order and anti-ferromagnetic phase, we apply the model to a bipartite lattice where we distinguished two different sub-lattices (A and B) forming a NaCl-like structure. The Hamiltonian reads as expressed in Equation 1.

$$H = -t\sum_{i,j,\sigma}\left(c^{\dagger}_{iA\sigma}c_{jB\sigma} + c^{\dagger}_{jB\sigma}c_{iA\sigma}\right) + U\sum_{i}\left(n_{iA\uparrow}n_{iA\downarrow} + n_{iB\uparrow}n_{iB\downarrow}\right) - \mu\sum_{i,\sigma}\left(n_{iA\sigma} + n_{iB\sigma}\right). \quad (1)$$

The first term represents hopping of electrons between nearest-neighbor sites of different sub-lattices with the hopping parameter t. The indices (i,j) represent unit cells, while (A, B) represent sub-lattices, and σ denotes the spin component of electrons. The second term corresponds to the on-site Coulomb repulsion, with U being the corresponding parameter. The third term is introduced to control the filling, where μ is the chemical potential. Here $n_{iA(B)\sigma} = c^{\dagger}_{iA(B)\sigma}c_{iA(B)\sigma}$, is occupation number operator of electrons occupying unit cell i and sublattice $A(B)$ with a spin component σ.

2.2 Method of Calculation

In this work, we proposed a new approach as an impurity solver within dynamical mean field theory framework. We started by using the standard dynamical mean field algorithm, where we defined an initial guess of the self-energy matrix $[\Sigma(z)]$, with $z = i\omega_n + \mu$ (in the Matsubara-frequency domain), or $z = \omega + i0^{+}$ (in the real-frequency domain). Here, $\omega_n = (2n+1)\pi k_B T$, with $n = \cdots, -2, -1, 0, 1, 2, \ldots$ is the fermionic Matsubara frequency [8]. We defined the Green function matrix through the Dyson equation as expressed in Equation 12-4.

$$[G(\boldsymbol{k}, z)] = [z - [H_0(\boldsymbol{k})] - \Sigma(z)]^{-1}. \quad (2)$$

The Green function matrix was then averaged over $\boldsymbol{k}$-points in the Brillouin zone

$$\overline{[G(z)]} = \frac{1}{N}\sum_{\boldsymbol{k}}[G(\boldsymbol{k}, z)]. \quad (3)$$

Next, we extracted the mean-field Green function matrix through

$$[G(z)]_{\mathrm{MF}} = \left[\overline{[G(z)]}^{-1} + [\Sigma(z)]\right]^{-1}. \quad (4)$$

At this step, we entered the new impurity solver we were proposing. The expression of the interaction term can be written as expressed in Equation 5.

$$U\sum_i (n_{iA\uparrow}n_{iA\downarrow} + n_{iB\uparrow}n_{iB\downarrow}) = \frac{U}{2}\sum_i (n_{iA\uparrow}n_{iA\downarrow} + n_{iA\uparrow}n_{iA\downarrow} + n_{iB\uparrow}n_{iB\downarrow} + n_{iB\uparrow}n_{iB\downarrow})$$
$$= \frac{U}{2}\sum_i [n_{iA\uparrow}(\langle n_{iA\downarrow}\rangle + \delta_{iA\downarrow}) + (\langle n_{iA\uparrow}\rangle + \delta_{iA\uparrow})n_{iA\downarrow} + (\langle n_{iB\uparrow}\rangle + \delta_{iB\uparrow})n_{iB\downarrow} + n_{iB\uparrow}(\langle n_{iB\downarrow}\rangle + \delta_{iB\downarrow})] \quad (5)$$

where we treated the occupancy fluctuations ($\delta_{iA(B)\sigma}$) as classical quantities that we varied continuously between $(1-\langle n_{i\sigma}\rangle)$ and $(-\langle n_{i\sigma}\rangle)$. We then defined the local self-energy matrix that carried the dependence on the average occupancies and their fluctuations as expressed in Equation 6.

$$[\Sigma(\langle n_{A\downarrow}\rangle, \langle n_{A\uparrow}\rangle, \langle n_{B\downarrow}\rangle, \langle n_{B\uparrow}\rangle, \delta_{A\uparrow}, \delta_{A\downarrow}, \delta_{B\uparrow}, \delta_{B\downarrow})]_{\text{loc}} =$$
$$\frac{U}{2}\begin{bmatrix} (\langle n_{A\downarrow}\rangle + \delta_{A\downarrow}) & 0 & 0 & 0 \\ 0 & (\langle n_{A\uparrow}\rangle + \delta_{A\uparrow}) & 0 & 0 \\ 0 & 0 & (\langle n_{A\uparrow}\rangle + \delta_{A\uparrow}) & 0 \\ 0 & 0 & 0 & (\langle n_{B\downarrow}\rangle + \delta_{B\downarrow}) \end{bmatrix}, \quad (6)$$

where we have dropped the unit cell index i as the expression holds for each unit cell.

From the local self-energy matrix, we could construct the local interacting Green function matrix as expressed in Equation 7.

$$[G(z, \langle n_{A\downarrow}\rangle, \langle n_{A\uparrow}\rangle, \langle n_{B\downarrow}\rangle, \langle n_{B\uparrow}\rangle, \delta_{A\uparrow}, \delta_{A\downarrow}, \delta_{B\uparrow}, \delta_{B\downarrow})]_{\text{loc}} = [[G(z)]_{\text{MF}}{}^{-1} - \Sigma(\langle n_{A\downarrow}\rangle, \langle n_{A\uparrow}\rangle, \langle n_{B\downarrow}\rangle, \langle n_{B\uparrow}\rangle, \delta_{A\uparrow}, \delta_{A\downarrow}, \delta_{B\uparrow}, \delta_{B\downarrow})]_{\text{loc}}]^{-1}. \quad (7)$$

Further, we constructed the effective action as expressed in Equation 8.

$$S_{\text{eff}}(\langle n_{A\downarrow}\rangle, \langle n_{A\uparrow}\rangle, \langle n_{B\downarrow}\rangle, \langle n_{B\uparrow}\rangle, \delta_{A\uparrow}, \delta_{A\downarrow}, \delta_{B\uparrow}, \delta_{B\downarrow})_{\text{eff}} = -\sum_n \ln\left|[G(z)]_{\text{MF}}{}^{-1}[G(z, \langle n_{A\downarrow}\rangle, \langle n_{A\uparrow}\rangle, \langle n_{B\downarrow}\rangle, \langle n_{B\uparrow}\rangle, \delta_{A\uparrow}, \delta_{A\downarrow}, \delta_{B\uparrow}, \delta_{B\downarrow})]_{\text{loc}}\right| e^{i\omega_n 0+} \quad (8)$$

From the effective action, we could define the statistical weighting factor (P) and the partition function (Z) as expressed in Equation 9-10.

$$P(\langle n_{A\downarrow}\rangle, \langle n_{A\uparrow}\rangle, \langle n_{B\downarrow}\rangle, \langle n_{B\uparrow}\rangle, \delta_{A\uparrow}, \delta_{A\downarrow}, \delta_{B\uparrow}, \delta_{B\downarrow}) = \frac{1}{Z}\exp\{-S_{\text{eff}}(\langle n_{A\downarrow}\rangle, \langle n_{A\uparrow}\rangle, \langle n_{B\downarrow}\rangle, \langle n_{B\uparrow}\rangle, \delta_{A\uparrow}, \delta_{A\downarrow}, \delta_{B\uparrow}, \delta_{B\downarrow})_{\text{eff}}\} \quad (9)$$

$$Z = \int d\delta_{A\uparrow}\int d\delta_{A\downarrow}\int d\delta_{B\uparrow}\int d\delta_{B\downarrow}\ P(\langle n_{A\downarrow}\rangle, \langle n_{A\uparrow}\rangle, \langle n_{B\downarrow}\rangle, \langle n_{B\uparrow}\rangle, \delta_{A\uparrow}, \delta_{A\downarrow}, \delta_{B\uparrow}, \delta_{B\downarrow}). \quad (10)$$

The weighting factor was used to average the local interacting Green function matrix over all possible values of occupancy fluctuations through Equation 11

$$[G(z)]_{\text{ave}} = \int d\delta_{A\uparrow}\int d\delta_{A\downarrow}\int d\delta_{B\uparrow}\int d\delta_{B\downarrow}\, P(\langle n_{A\downarrow}\rangle, \langle n_{A\uparrow}\rangle, \langle n_{B\downarrow}\rangle, \langle n_{B\uparrow}\rangle, \delta_{A\uparrow}, \delta_{A\downarrow}, \delta_{B\uparrow}, \delta_{B\downarrow}) \quad (11)$$
$$\left[G\left(z, (\langle n_{A\downarrow}\rangle, \langle n_{A\uparrow}\rangle, \langle n_{B\downarrow}\rangle, \langle n_{B\uparrow}\rangle, \delta_{A\uparrow}, \delta_{A\downarrow}, \delta_{B\uparrow}, \delta_{B\downarrow})\right)\right]_{\text{loc}},$$

from which we could re-calculate the self-energy matrix as expressed in Equation 12.

$$[\Sigma(z)] = [G(z)]_{\text{MF}}{}^{-1} - [G(z)]_{\text{ave}}{}^{-1}. \quad (12)$$

We then checked the convergence by comparing the initial guess and the recalculated self-energy matrices, and iterated the entire steps until the convergence was achieved. We must perform the

iterations in both the Matsubara and real-frequency domains, where the real-frequency loop may be placed inside the Matsubara-frequency loop, with the sequence being exactly the same for both loops, except that the statistical weighting factor (P) is only computed in the Matsubara-frequency domain.

From the averaged Green function in Eq. (2) or Eq. (11) in the real-frequency domain, we could calculate the density of states (DOS) as

$$\mathrm{DOS}(\omega) = -\frac{1}{\pi}\mathrm{Im}\mathrm{Tr}[G(\omega + i0^+)]. \tag{13}$$

The chemical potential value μ may be guessed in the initial step in Eq. (1), but needed to be updated throughout the iterations by imposing the total occupancy constraint corresponding to the quarter-filled system, that is

$$\langle n \rangle = \langle n_{A\uparrow} \rangle + \langle n_{A\downarrow} \rangle + \langle n_{B\uparrow} \rangle + \langle n_{B\downarrow} \rangle = 1 \tag{14}$$

with

$$\langle n_{\lambda\sigma} \rangle = \int d\omega \, \mathrm{PDOS}_{\lambda\sigma}(\omega) f(\omega, \mu, T) \tag{15}$$

being the average electron occupancy at sub-lattice λ with spin σ, and the projected DOS (PDOS) being defined as

$$\mathrm{PDOS}_{\lambda\sigma} = -\frac{1}{\pi}\mathrm{Im}G_{\lambda\sigma}(\omega + i0^+). \tag{16}$$

The calculated $\langle n_{\lambda\sigma} \rangle$ was used in the computation of new local self-energy matrix elements in Eq. (6). We iterated all the above steps until the convergence was achieved.

3. Results and Discussion

For our calculations, we set the hopping parameter fixed at t = 1 eV. First, we studied how the DOS evolved as we varied U at a fixed low-temperature value T = 50 K. The results are shown in Figure 1. We saw that $U = 3$ eV was a very shallow pseudogap just started to appear (below this U value, no noticeable pseudogap was observed). As we increased U with T kept fixed, the pseudogap became more noticeable and eventually became almost a full gap at $U \geq 5$ eV. Note that all the DOS curves were plotted with respect to $\omega - \mu$. Hence, the condition of $\omega - \mu = 0$ marked the position of the chemical potential. From the figure, we can see that as the pseudogap developed until it became almost a full gap, the chemical potential stayed outside the pseudogap or the gap region. This means that the formation of the gap did not lead the system to transform into an insulator. In other words, the system remained a metal. As a comparison, in the case of half filling, the standard 3D Hubbard model for large U revealed the gap into which the chemical potential falled. This means that each electron tended to localize at a site, effectively resulting no electron being itinerant [8].

Next, for the relatively large U values where the system had established almost a full gap, we varied the temperature T and showed how the DOS evolved with the temperature. Figure 2(a) and 2(b) show the evolution of DOS as a function of temperature for $U = 5$ eV and $U = 6$ eV, respectively. As the temperature increased, we observed that the pseudogap tended to become more shallow and eventually disappeared. These results seemed to hold generally for all variants of the Hubbard model at high temperatures [8].

At this point, we would like to comment that, to the best of our knowledge, there is not much existing literature that shows explicitly the density of states away from half filling or specifically at quarter filling. The closest match to our model is Ref. [9], where at Figure 10, it shows the density of states for a system away from half filling in which there existed a pseudogap with the chemical potential lying outside the pseudogap. This is consistent with the behavior shown by our density of states results that characterizes the system as a metal.

In addition to studying the evolution of DOS, we also studied the possibility of formation of an ordered phase in this model by computing the corresponding order parameter. In this study, we inspected the ferromagnetic order parameter,

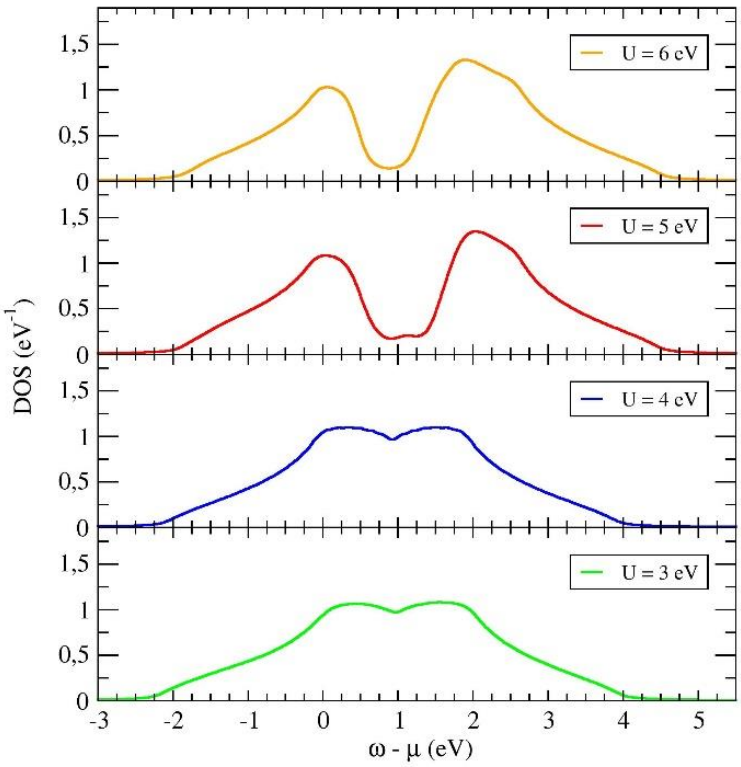

Figure 1. The density of states for various U values at fixed temperature T = 50 K

$$m = (\langle n_{A\uparrow}\rangle + \langle n_{B\uparrow}\rangle) - (\langle n_{A\downarrow}\rangle + \langle n_{B\downarrow}\rangle), \tag{17}$$

the ferromagnetic order parameter,

$$m_{\text{staggered}} = (\langle n_{A\uparrow}\rangle - \langle n_{A\downarrow}\rangle) + (\langle n_{B\downarrow}\rangle - \langle n_{B\uparrow}\rangle), \tag{18}$$

and the charge order parameter,

$$\text{CO} = (\langle n_{A\uparrow}\rangle + \langle n_{A\downarrow}\rangle) - (\langle n_{B\uparrow}\rangle + \langle n_{B\downarrow}\rangle). \tag{19}$$

Our results were zero for all the above order parameters for all U and T values indicating that the system represented by the 3D Hubbard model at quarter filling was always in the paramagnetic phase. As far as our knowledge, the charge ordering phase has been reported in the extended Hubbard model, that is the Hubbard model that includes the intersite Coulomb repulsion, which is not the same as the model we present here.

Overall, our calculations basically revealed the same physics known to exist in the 3D Hubbard model at quarter filling. This suggests that our algorithm can be a legitimate alternative impurity solver for the Hubbard model within DMFT. In addition to the potentially less computational cost compared to other more sophisticated methods, this new algorithm may offer a more convenient way to compute the dynamical (i.e. frequency dependent) quantities, as the algorithm allows one to directly harvest the retarded Green function from the self-consistent proces. With this, we did not need to do analytic continuation numerically as it might be needed by other DMFT methods, such as Quantum Monte Carlo [6].

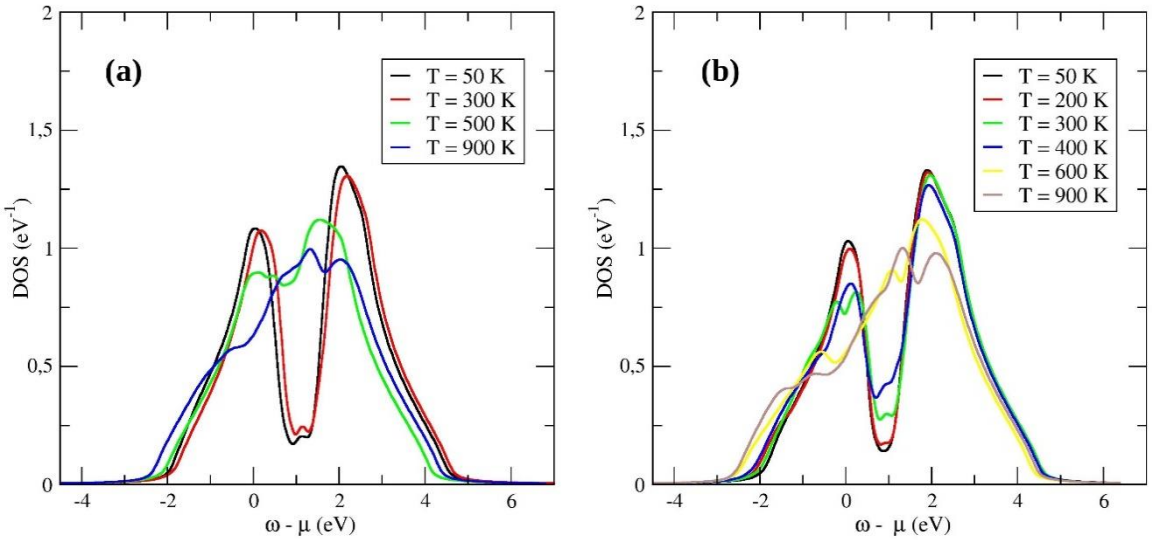

Figure 2. The density of states for (a) U = 5 eV and (b) U = 6 eV for various temperatures

4. Conclusion

We have demonstrated a new algorithm of DMFT impurity solver for 3D Hubbard model at a quarter filling, based on treating the occupancy fluctuations semiclassically. We tested our algorithm by evaluating the DOS for various U values at a fixed temperature, and for the various temperatures at fixed U values. As U increased at a fixed temperature, the DOS formed a pseudogap that became deeper and wider with the increasing U. Meanwhile, by varying temperature for various temperatures at a fixed U, the pseudogap in the DOS tended to become more shallow and eventually diminish at very high temperatures. We also inspected the possibility of some ordered phase formations, and have found that the system remained in the paramagnetic metallic phase for all U values and temperatures. All these results are consistent with those reported in the literature relevant for 3D Hubbard model at quarter filling. Besides offering a potentially cheaper computation, our algorithm may also offer a convenient way to compute the dynamical quantities as it does not need to employ numerical analytic continuation process. After all, further development of the method remains necessary to check its general validity for a broader spectrum of model parameters.

References

[1] Imada M, Fujimori A and Tokura Y 1998 Metal-insulator transitions *Reviews of Modern Physics* **70** 1039–263
[2] Verwey E J W 1939 Electronic Conduction of Magnetite (Fe3O4) and its Transition Point at Low Temperatures *Nature* **144** 327–8
[3] Verwey E J W and Haayman P W 1941 Electronic conductivity and transition point of magnetite ("Fe_3O_4") *Physica* **8** 979–87
[4] Richard T. Scalettar, Pavarini E, Koch E, Brink J van den, Sawatzky G, Institute for Advanced Simulation and German Research School for Simulation Sciences 2016 *Quantum materials: experiments and theory: lectures notes of the Autumn School on Correlated Electrons 2016 : at Forschungszentrum Jülich, 12-16 September 2016*
[5] Dagotto E 1994 Correlated electrons in high-temperature superconductors *Reviews of Modern Physics* **66** 763–840
[6] Georges A, Kotliar G, Krauth W and Rozenberg M J 1996 Dynamical mean-field theory of strongly correlated fermion systems and the limit of infinite dimensions *Reviews of Modern Physics* **68** 13–125

[7] Millis A J 1996 Cooperative Jahn-Teller effect and electron-phonon coupling in $La_{1-x}A_xMnO_3$ *Physical Review B* **53** 8434–41
[8] Anisimov V I, Poteryaev A I, Korotin M A, Anokhin A O and Kotliar G 1997 First-principles calculations of the electronic structure and spectra of strongly correlated systems: dynamical mean-field theory *Journal of Physics: Condensed Matter* **9** 7359–67
[9] Terletska H, Chen T, Paki J and Gull E 2018 Charge ordering and nonlocal correlations in the doped extended Hubbard model *Physical Review B* **97**

Acknowledgments
We thank Universitas Indonesia for supporting this research project with a full funding through PITTA Research Grant No. 2286/UN2.R3.1/HKP.05.00/2018.